Journal of Catalysis 274 (2010) 1–10

Contents lists available at ScienceDirect

Journal of Catalysis

journal homepage: www.elsevier.com/locate/jcat

Low-temperature CO oxidation over supported Pt, Pd catalysts: Particular role of FeO_x support for oxygen supply during reactions

Lequan Liu [a,b], Feng Zhou [a], Liguo Wang [a], Xiujuan Qi [a], Feng Shi [a], Youquan Deng [a,*]

[a] Centre for Green Chemistry and Catalysis, Lanzhou Institute of Chemical Physics, Chinese Academy of Sciences, Lanzhou 730000, China
[b] Graduate University of Chinese Academy of Sciences, Beijing 100049, China

ARTICLE INFO

Article history:
Received 7 March 2010
Revised 18 May 2010
Accepted 20 May 2010
Available online 8 July 2010

Keywords:
CO oxidation
Pt catalyst
Pd catalyst
Kinetic measurements
Strong metal–support interaction (SMSI) effect
Oxygen vacancy
H_2–O_2 titration
Time-resolved CO titration

ABSTRACT

A series of FeO_x- and Al_2O_3-supported Pt, Pd catalysts (0.23–2.1%) were prepared in this study. Pt/FeO_x exhibited high CO oxidation activity with turnover frequency of 151×10^{-3} s^{-1} (1% CO balanced with air, atmospheric pressure, 27 °C). A systematical study of FeO_x- and Al_2O_3-supported Pt, Pd catalysts by means of X-ray photoelectron spectroscopy, X-ray diffraction, high-resolution transmission electron microscopy, temperature-programmed reduction, H_2–O_2 titration, and time-resolved CO titration is reported. From 7% to 39% of Fe^{3+} was reduced to Fe^{2+} over $Fe(OH)_x$-supported Pd and Pt catalysts, accompanied by Pd, Pt hydrogenation and hydroxyl loss, and a large amount of oxygen vacancies were proposed to be produced. Results of H_2–O_2 titration and time-resolved CO titration showed that a large amount of oxygen adsorbed onto FeO_x support in the presence of Pt, Pd. This made CO oxidations over Pt/FeO_x, Pd/FeO_x proceed over two adjacent but different active sites (Pt, Pd for CO and FeO_x for oxygen) with low apparent activation energies (30–34 kJ/mol), which accounted for their high activity in low-temperature CO oxidation.

1. Introduction

Catalytic oxidation of CO has been studied extensively because of its great importance for both practical applications and fundamental research, e.g., gas masks, purification of hydrogen for proton-exchange membrane fuel cells (PEMFCs) [1]. Among various heterogeneous catalysts involved, supported metals, especially noble metals—e.g., Pt, Pd, Au, and Ru nanocatalysts—show prominent properties. After the seminal discovery of high catalytic activity of supported Au catalysts for low-temperature CO oxidation [2], more extensive studies of CO oxidation were carried out [3,4]. For CO oxidation, it is generally accepted that supported Au catalysts are more active at lower temperatures, while the turnover frequencies (TOFs) of supported Pt and Pd catalysts are much higher above 200 °C [5]. This is understandable, as CO is strongly and almost exclusively adsorbed onto Pt and Pd, resulting in the unavailability of active oxygen, which is essential for low-temperature CO oxidation. Hence, low-temperature CO oxidation over those catalysts proceeds in a competitive Langmuir–Hinshelwood way characterized by high apparent activation energies (E_a) [6,7]. Thus, supported Pt catalysts are traditionally considered to be almost inert in low-temperature CO oxidation. On the other hand, supported Pt catalysts as the most ideal electrode materials in PEMFCs are often poisoned with CO. Thus, pursuing high activity of CO oxidation over Pt catalysts or at least CO-tolerant electrode Pt catalysts and further understanding the mechanism are of great interest and importance.

It is well known that supports, preparation methods, and promoters are of great importance in preparing highly active catalysts. Any modification or adjustment may result in unexpected catalytic behavior. Regarding preferential CO oxidation over supported Pt, Pd catalysts, there have been plenty of investigations on the effects of promoters [8–14]. However, with respect to low-temperature CO oxidation, Pt and Pd catalysts with relatively high activity have seldom been reported [15–17]. For example, the temperature at which CO was totally converted over Fe-promoted PtFe/SiO_2 (1% Pt, 0.055% Fe) was 140 °C, while this temperature was 230 °C over traditional 1% Pt/SiO_2 prepared by incipient wetness impregnation (1% CO, balance with air, GHSV of 120,000 ml g^{-1} h^{-1}) [18]. Recently, we have found for the first time that ferric-hydroxide-supported Pd catalyst prepared by co-precipitation without calcination at elevated temperatures exhibits high activity (0.17 $mmol_{CO}$ g_{Pd}^{-1} s^{-1} at 27 °C) in low-temperature CO oxidation [19]. Li et al. reported that Pt/Fe_2O_3 prepared by a colloid-deposition method under wet conditions was relatively active for CO oxidation [20]. However, the reason those supported Pt and Pd catalysts exhibited unusual activity for low-temperature CO oxidation

* Corresponding author. Fax: +86 931 4968116.
E-mail address: ydeng@licp.cas.cn (Y. Deng).

0021-9517/$ - see front matter © 2010 Elsevier Inc. All rights reserved.
doi:10.1016/j.jcat.2010.05.022

is unclear. In this work, FeO_x-supported Pt was prepared to confirm the generality of our reported method, and high catalytic activity (151×10^{-3} s^{-1}, 1% CO balanced with air, atmospheric pressure, 27 °C) in low-temperature CO oxidation was obtained. To gain insight into why catalysts prepared in this manner possessed high activity, we carried out systematic characterizations over FeO_x-, Fe_2O_3-, and Al_2O_3-supported Pt, Pd, including kinetic measurements, X-ray photoelectron (XPS) spectroscopy, X-ray diffraction (XRD), high-resolution transmission electron microscopy (HRTEM), temperature-programmed reduction (TPR), H_2–O_2 titration (HOT), and time-resolved CO titration. This leads to the conclusion that FeO_x in the presence of Pt, Pd could supply active oxygen, which can react with CO, and a speculated mechanism involving FeO_x support is derived.

2.Experiment

2.1. Catalyst preparation

A series of $Fe(OH)_x$-, FeO_x-, and Fe_2O_3-supported Pt catalysts was prepared by a co-precipitation method. An aqueous mixture of 0.1 g/ml $H_2PtCl_6{\cdot}6H_2O$ with 1.0 mol/L $Fe(NO_3)_3$ was added dropwise to 1 mol/L Na_2CO_3 solution under stirring, and the final pH was controlled to ca. 8.5. After the solution was stirred and aged for 3 h, the resulting precipitates were filtered, washed several times with distilled water, and dried at 80 °C for 8 h in an oven. Subsequently, the resulting brown powders were treated at 200 °C for 5 h or at 500 °C for 4 h in static air; the products were denoted as $Pt/Fe(OH)_x$ and Pt/Fe_2O_3-NR (nonreduced), respectively. Subsequently, $Pt/Fe(OH)_x$ and Pt/Fe_2O_3-NR were respectively further reduced at 200 °C for 2 h and 300 °C for 2 h with pure H_2; the products were denoted as Pt/FeO_x and Pt/Fe_2O_3. $Fe(OH)_x$-, FeO_x-, and Fe_2O_3-supported Pd catalysts were prepared in a similar manner except for heating and reducing temperatures. For pertinent comparison with our early report [19], $Pd/Fe(OH)_x$ was reduced at 80 °C for 2 h directly after being dried at 80 °C for 8 h, denoted as Pd/FeO_x. $Pd/Fe(OH)_x$ was calcined at 500 °C for 4 h in static air and reduced with H_2, denoted as Pd/Fe_2O_3. Au/FeO_x catalyst was prepared by a method similar to that for Pt/FeO_x without reduction, and 4.4 wt% Au/Fe_2O_3 bought from the World Gold Council (denoted as Au/Fe_2O_3-W) was also employed. For comparison, Pt/Al_2O_3 and Pd/Al_2O_3 catalysts prepared by incipient wetness impregnation were also tested. Generally, γ-Al_2O_3 (80–100 mesh) was calcined at 600 °C for 4 h before the introduction of Pt or Pd. Pt/Al_2O_3-NR (nonreduced), and Pd/Al_2O_3-NR (nonreduced) was prepared by impregnating Al_2O_3 with $H_2PtCl_6{\cdot}6H_2O$ or $PdCl_2$ solution. The mixture was stirred, and then the water was removed under reduced pressure at about 65 °C. The catalysts were dried at 120 °C, calcined in air at 500 °C for 4 h, and reduced with pure H_2 at 500 °C for 2 h, denoted as Pt/Al_2O_3 and Pd/Al_2O_3, respectively. All chemicals were used as received (A.R.) without further purification.

2.2. Catalyst characterization

Pt, Pd, and Au loadings in the catalyst samples were measured by atomic absorption spectroscopy (AA240, Varian). BET surface areas (SBET) were obtained by physisorption of N_2 at 77 K with a Micromeritics ASAP 2010. It must be pointed out that the Pd/FeO_x catalyst samples were outgassed to 0.1 Pa at 80 °C to ensure no change in the support structure. The other catalysts were outgassed to 0.1 Pa at 200 °C.

XRD measurements for structure determination were carried out on a Siemens D/max-RB powder X-ray diffractometer. Diffraction patterns were recorded with Cu Kα radiation (40 mA, 40 kV) over a 2θ range of 15–75° and a position-sensitive detector using a step size of 0.01° and a step time of 0.15 s.

XPS analyses were performed with a VG ESCALAB 210 instrument. Mg Kα radiation at an energy scale calibrated versus adventitious carbon (C1*s* peak at 284.8 eV) was used. The sample powders were pelletized and then mounted on double-sided adhesive tape. The pressure in the analysis chamber was in the range of 10^{-9} Torr during data collection and the sample was kept at such a low pressure for 24 h without heating before being analyzed. The surface compositions of the samples were determined from the peak areas of the corresponding origin fitting lines.

HRTEM investigations were carried out with a JEOL JEM-2010 electron microscope. The powdered catalysts were suspended in toluene with ultrasonic dispersion for 5–10 min and then the resulting solution was dropped on a holey carbon film supported by a 300-mesh copper grid.

2.3. Catalyst activity tests and kinetic measurements

Catalytic activity measurements were carried out in a fixed-bed reactor at atmospheric pressure with 10–40 mg of catalyst, which was diluted with chemically inert α-Al_2O_3. The feed gas for the oxidation was about 1 vol% CO balanced with air (without further purification). Measurements were performed under differential reaction conditions. To limit the conversion to values typically between 5% and 25%, a flux of 25–50 ml/min at 5–220 °C for different catalysts was used. All data were acquired after 60 min reaction time. The concentrations of CO and O_2 in the effluent gas were analyzed on-line by a gas chromatograph equipped with a thermal conductivity detector (TCD) using Ar as carrier gas. The conversion of CO was calculated from the change in CO concentration between the inlet and outlet gases. For comparison of catalytic activity, two parameters are used: reaction rates in $mmol_{CO}\ mol_M^{-1}\ s^{-1}$ (M: Pt, Pd, and Au), which were obtained from differential reaction results, and TOFs, which were obtained based on surface metal atoms from CO chemisorption.

2.4. TPR, CO pulse chemisorption, H_2–O_2 titration, and time-resolved CO titration

TPR experiments were preformed in a catalyst-characterization-system equipped with a TCD. Generally, TPR measurements were conducted as follows: 80 mg catalyst powder (80–100 mesh) was first charged; after pretreatments with air and purging with highly pure N_2 for 1 h at selected temperatures (at which catalysts were heat-treated in the preparation procedure), the samples were cooled down to room temperature, and then reduced with 5% H_2 balanced with N_2 at a rate of 10 °C/min.

Measurement of the accessible metal area by CO pulse chemisorption was carried out at room temperature by a pulse injection method following the same experimental and data handling procedures as in early reports [21,22]. In principle, samples were first purged with nitrogen for 30 min, and then pure H_2 was introduced into the system and catalysts were reduced at selected temperatures. CO pulses (0.1727 ml) were injected into the carrier gas intermittently after the sample was cooled to room temperature, and the whole process was detected by a TCD. In calculating Pt- and Pd-specific surface areas from CO chemisorption data, it was assumed that CO was chemisorbed in a bridged form over Pd atoms and in a line form over Pt atoms.

HOT and time-resolved CO titration experiments were preformed in a catalyst-characterization-system equipped with a quadrupole mass spectrometer (DM 300, AMETEK, USA). O_2–H_2 or H_2–O_2 titration measurements were carried out at selected temperatures (Pt/FeO_x at 40 °C, Pd/FeO_x and Pd/Al_2O_3 at 80 °C, Pt/Al_2O_3 at room temperature). Qualitative and quantitative analysis was

conducted in a mass spectrometer (MS). The carrier gas as well as the reducing gas was strictly deoxidized before being introduced into the dynamic system. For O_2–H_2 titrations, catalyst samples were first reduced in an H_2 stream and purged with highly pure N_2 for 1 h. After samples were cooled to selected temperatures, O_2 pulses (0.1727 ml) were introduced into the carrier gas until total saturation. After the sample was purged with N_2 for 30 min, the adsorbed oxygen was titrated by introducing pulses of hydrogen to give HOT-H_T. H_2–O_2 titrations were conducted in a similar manner except for the pulse order: samples were first saturated with hydrogen and then titrated with oxygen to give HOT-O_T.

Time-resolved CO titrations were carried out as follows: an 80-mg sample was reduced in situ with 5% H_2/Ar and then purged with deoxidized Ar. After being cooled to selected temperatures (150 °C for Pt/Al_2O_3 and 25 °C for Pt/FeO_x), the sample was either saturated with 1% O_2/Ar for 20 min or not and was purged with Ar for 30 min in order to remove the residual gas-phase O_2. Subsequently, 1% CO in Ar was introduced, and both CO and CO_2 responses were recorded with MS detector.

3. Results and discussion

Data from characterization of the catalysts used, such as noble metal loadings and BET surface areas, are summarized in Table 1. FeO_x-supported catalysts possessed relatively higher BET surface (70–150 m^2/g), while surface area decreased greatly to about 30 m^2/g after catalysts were treated at 500 °C. As expected, Al_2O_3-supported Pt and Pd catalysts possess relatively high BET surface areas (~200 m^2/g), though also treated at high temperatures.

3.1. The catalytic activities and kinetic study of CO oxidation over supported Pt and Pd catalysts

First, the active test system was benchmarked with the standard catalyst 4.4 wt% Au/Fe_2O_3-W. In our active test system, the temperature at 50% CO conversion is −30 °C, which is slightly higher than the provided temperature of −37 °C (100 mg, flow rate of 33 ml/min, space velocity (SV) 20,000 ml h^{-1} g^{-1}), indicating that our active test system is reliable.

All pure supports were first tested at a feed gas flow rate of 20 ml/min, which resulted in a SV of 15,000 ml g_{cat}^{-1} h^{-1}, and they required much higher temperatures compared to light-off of corresponding catalysts. Therefore, their contribution to the overall conversions could easily be neglected. Arrhenius-type plot experiments were carried out at atmospheric pressure with 1% CO (balanced with air). The fractional conversions of CO over Pt/FeO_x, Pt/Fe(OH)$_x$, Pt/Fe_2O_3, Pd/Fe(OH)$_x$, Pd/Fe_2O_3, and Pd/FeO_x were between 0.05 and 0.25 at all temperatures studied. For Pt/Al_2O_3 and Pd/Al_2O_3, the fractional conversion of CO was between 0.05 and 0.25 at temperatures below 160 °C, and ⩽0.4 at 190 °C and 210 °C. First, 1.5% Pt/Al_2O_3 and 1.4% Pd/Al_2O_3 were tested. As can be seen from Fig. 1, those two catalysts show hardly any activity at temperatures below 50 °C. Reaction rates of 8.5 $mmol_{CO}$ mol_{Pt}^{-1} s^{-1} and 3.2 $mmol_{CO}$ mol_{Pd}^{-1} s^{-1}, respectively, were obtained at 130 °C, which is consistent with early reports [6,23]. This is reasonable, as CO strongly and almost exclusively adsorbs onto Pt and Pd sites, resulting in no active sites for O_2 activation at low temperatures. With increasing temperature, Pt and Pd sites become available for O_2 adsorption, which can then offer active oxygen for CO oxidation. However, the 1.5% Pt/FeO_x and 1.9% Pd/FeO_x catalysts exhibited unexpected high activity for low-temperature CO oxidation. A reaction rate of 26 $mmol_{CO}$ mol_{Pt}^{-1} s^{-1} was obtained at 27 °C over 1.5% Pt/FeO_x catalyst, and it increased to 31 $mmol_{CO}$ mol_{Pt}^{-1} s^{-1} when the Pt content decreased to 0.23% (not shown here). That is, the activity over Pt/FeO_x, though with lower surface area, is distinctly superior to that over 1.5% Pt/Al_2O_3 (almost no activity at 27 °C), indicating that BET surface area does not have a direct relationship with catalytic activity. As for Pd/FeO_x, a reaction rate of 16 $mmol_{CO}$ mol_{Pd}^{-1} s^{-1} (27 °C) was obtained, which was in accordance with our earlier report [19]. For unreduced catalysts in which Pt and Pd were in oxidized states, reaction rates of 5.1 $mmol_{CO}$ mol_{Pt}^{-1} s^{-1} (130 °C) and 5.9 $mmol_{CO}$ mol_{Pd}^{-1} s^{-1} (50 °C) were obtained over Pt/Fe(OH)$_x$ and Pd/Fe(OH)$_x$, respectively, indicating that the reduction procedure was more important for Pt/FeO_x. After being treated at 500 °C for 4 h and reduced at 300 °C, 1.6% Pt/Fe_2O_3 exhibited an obvious activity decrease in CO oxidation: the reaction rate decreased to 3.2 $mmol_{CO}$ mol_{Pt}^{-1} s^{-1} (27 °C). As for Pd/Fe_2O_3, a reaction rate of only 0.4 $mmol_{CO}$ mol_{Pd}^{-1} s^{-1} (27 °C) was obtained, indicating that FeO_x- or Fe_2O_3-supported Pd catalysts were more easily affected by calcination than supported Pt catalysts. A similar activity decrease after calcination has been reported previously [24–26]. As supported Au catalysts are generally accepted as suitable catalysts for low-temperature CO oxidation, 4.4 wt% Au/Fe_2O_3-W from the World Gold Council and 2.0 wt% Au/FeO_x prepared by the same method as 1.5% Pt/FeO_x were also tested for comparison. Reaction rates of 5.9 $mmol_{CO}$ mol_{Au}^{-1} s^{-1} (27 °C) and 120 $mmol_{CO}$ mol_{Au}^{-1} s^{-1} (27 °C) were obtained respectively over those two supported Au catalysts.

To gain insight into the intrinsic activities of supported Pt, Pd, and Au catalysts, TOFs normalized by the number of surface noble metal atoms were compared (Table 2). TOFs were derived from differential reaction results. The 1.5% Pt/FeO_x gave a TOF of 151×10^{-3} s^{-1} at 27 °C (300 K), exhibiting significantly higher catalytic activity than 1.5% Pt/Al_2O_3 (34.2×10^{-3} s^{-1}, 130 °C) prepared by traditional incipient wetness impregnation. Meanwhile, it was also superior to 4.4 wt% Au/Fe_2O_3-W (20.3×10^{-3} s^{-1}, 27 °C). However, FeO_x-supported Pt and Pd catalysts are both less active than 2.0 wt% Au/FeO_x (TOF of 400×10^{-3} s^{-1}, 27 °C), which was prepared in a manner similar to Pt/FeO_x. When we calculated the number of gold sites available, we made an estimate of 29% Au dispersion over 4.4 wt% Au/Fe_2O_3-W (based on 4-nm particles, as typically observed on Fe_2O_3 supports) [27]. By referring to meticulous HRTEM evaluation work by Herzing et al. [3], 30% Au dispersion over 2.0 wt% Au/FeO_x was used, as it has been evidenced that subnanometer clusters represent only 1.05 ± 0.72 atomic% of the total Au loading in those catalysts. Additionally, considering the encapsulation effect of FeO_x and the possibility of Pt–Fe bimetal formation as suggested by Rachmady and Vannice [28], a relatively low dispersion of Pt over 1.5% Pt/FeO_x (17.2%) was acceptable. Those results showed that the activities of FeO_x-supported Pt catalysts for CO oxidation, though slightly inferior, may be comparable to those of supported Au catalysts. This finding may change our traditional conception that supported Pt catalysts were extraordinary active for H_2 oxidation while they were nearly inert for low-temperature CO oxidation. It has been evidenced that obvious changes in particle size would occur through the growth of discrete nanoparticles or through agglomeration at elevated temperatures. Then it is reasonable to speculate that the decrease in activity may be partly caused by the increase in particle size, probably from clusters (~1 nm) to generalized nanoparticles. However, the distinct difference in catalytic activity over Pt and Pd on different supports (Al_2O_3 and FeO_x) may essentially come from complete different types of reaction mechanism.

The apparent activation energies of different catalysts and selected published results [29–31] for comparison are also presented in Table 2. As can be seen from the Arrhenius-type plots, Pt, Pd catalysts on different supports (FeO_x and Al_2O_3) show differences in E_a, Fig. 1. FeO_x-supported Pt, Pd catalysts showed almost the same E_a, 30 and 34 kJ/mol, respectively, suggesting that CO oxidation over those two catalysts proceeded by similar reaction pathways. Moreover, E_a of about 30 kJ/mol is close to that of supported Au catalysts, which have outstanding activity for low-temperature

Table 1
Some physicochemical properties of the supported Pt, Pd, and Au catalysts.

Catalyst	Pt/Pd/Au loadings (wt%)	BET surface area (m^2/g)	Average pore diameter (nm)	B.E. of Pd3$d_{5/2}$/Pt4$f_{7/2}$/Au4$f_{7/2}$ (eV)	Area ratio of M/M^{2+}[b]	B.E. of Fe 2$p_{3/2}$ (eV)	Atom ratio of Pt, Pd, or Au/Fe (from XPS)
$Fe(OH)_x$[a]	–	106	3.3	–	–	711.1	–
Pt/FeO_x	0.23	72.6	5.5	–	–	710.9	–
Pt/FeO_x	1.5	70	8.4	72.4, 71.3	0.68	711.0	0.01
Pt/Al_2O_3	1.5	203	10.1	72.5, 71.6	0.55	–	–
Pt/Fe_2O_3	1.6	25	7.7	72.7, 71.7	0.50	710.9	0.02
Pd/FeO_x	1.9	147	5.1	337.5, 335.7	0.58	711.1	0.04
Pd/Al_2O_3	1.4	193	8.6	337.1, 335.6	0.48	–	–
Pd/Fe_2O_3	2.1	30	6.4	337.9, 336.1	0.67	710.8	0.08
Au/FeO_x	2.0	85	9.0	83.9	–	710.9	0.01
Au/Fe_2O_3-W	4.4	39	–	83.6	–	710.7	0.03

[a] Support sample treated at 200 °C.
[b] M: Pt, Pd, or Au.

CO oxidation [32,33]. Nevertheless, Al_2O_3-supported Pt, Pd gave much higher activation energies, 115 and 71 kJ/mol, respectively. This is in good agreement with the literature results measured under similar conditions [34,35]. The striking difference in E_a suggested that the reaction pathways and/or rate-determining steps over those Al_2O_3-supported catalysts might be completely different when compared with FeO_x-supported Pt and Pd. Those results partly illustrated the fact that FeO_x-supported Pt and Pd catalysts exhibited superior CO oxidation activities when compared with Pt/Al_2O_3 and Pd/Al_2O_3. As mentioned earlier, strong and exclusive CO adsorption onto Pt or Pd active sites over Pt/Al_2O_3 and Pd/Al_2O_3 catalysts at low temperatures leads to the unavailability of active oxygen, while Al_2O_3 can hardly activate O_2 for CO oxidation, resulting in far inferior activity for low-temperature CO oxidation over those catalysts. Thus, to pursue highly active Pt, Pd catalysts, weakening the strength of CO adsorption on Pt and Pd or offering sites other than noble metal clusters as oxygen supply might be taken into account. Nevertheless, considering the large difference in E_a, it is reasonable to speculate that the dramatic activity difference between FeO_x- and Al_2O_3-supported Pt and Pd may more likely be caused by different CO oxidation mechanisms. As CO activation occurs over Pt active sites other than supports in those catalysts, the process of offering active oxygen might be different. That is, adsorption and activation of molecular oxygen could occur on FeO_x support but not on "inert" Al_2O_3. On the other hand, high-temperature calcined Fe_2O_3-supported Pt and Pd catalysts exhibited similar E_a when compared with Pt/FeO_x and Pd/FeO_x but with far inferior catalytic activity. This might be caused by the different CO oxidation mechanisms or pathways over those two kinds of catalysts (FeO_x- and Fe_2O_3-supported Pt, Pd), though the rate-determining step may be the same.

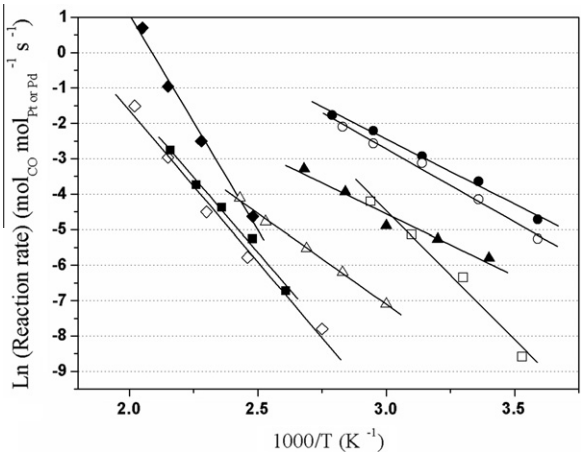

Fig. 1. Arrhenius plots of the reaction rate ln(r) vs. 1/T for CO oxidation over supported Pt, Pd catalysts. 1.5% Pt/Al_2O_3 (♦), 1.5% Pt/FeO_x (●), 1.3% $Pt/Fe(OH)_x$ (■), 1.6% Pt/Fe_2O_3 (▲), 1.4% Pd/Al_2O_3 (◇), 1.9% Pd/FeO_x (○), 1.7% $Pd/Fe(OH)_x$ (□), 2.1% Pd/Fe_2O_3 (△). Reaction conditions: 1.0 vol% CO in air, atmospheric pressure.

Fig. 2 shows the CO conversion over 1.5% Pt/FeO_x as a function of time at different SVs. At a relative high SV of 15,000 ml h^{-1} g^{-1}, the activity of Pt/FeO_x lasts just 60 min at 100% CO conversion, which is inferior to Pd/FeO_x, as we reported previously [19]. Nevertheless, at a SV of 7500 ml h^{-1} g^{-1}, total conversion of CO can be maintained for 6 h at 25 °C. Additionally, it could be prolonged to 9 h when the catalyst was subjected to a feeding gas of lower oxygen content (1% CO, 10% O_2, argon balance), indicating that the decrease in the catalytic activity might be caused by the change of Pt chemical states in the presence of O_2. That is, the reduced Pt state is more important for Pt/FeO_x than Pd/FeO_x, which is in accordance with the trend in catalytic performance of $Fe(OH)_x$-supported Pt, Pd before and after reduction. Further study on this issue is under way.

3.2. Chemical states and structural properties

Fig. 3 presents Pt4f photoelectron spectra obtained over Pt/FeO_x and Pt/Fe_2O_3 catalysts (the Pt4f spectrum of Pt/Al_2O_3 is not shown, as the Al2p peak is very strong and covers the Pt4f peaks completely). Fig. 4 shows the Pd3d photoelectron spectra of Pd/FeO_x and Pd/Al_2O_3. In Fig. 3a, the XP spectrum of Pt4f centers at 71.6 eV and shows broadened peaks with full widths at half maximum (FWHMs) of 2.5 eV, suggesting that it comprises Pt species with varying electronic states. After the Pt4f curve fitting, the spectrum consists of two pairs of peaks at 71.3 and 74.7 eV and at 72.4 and 75.6 eV, which are assigned to Pt^0 and Pt^{2+}, respectively. Such pairs of peaks were also found in Pt/Fe_2O_3 with a smaller fraction of Pt^0, which is also summarized in Table 1. Those results indicated that Pt was not fully reduced under the applied conditions. Note, however, that the binding energy of Pt4$f_{7/2}$ in the Pt/FeO_x catalyst shifts to a value lower (by 0.6 eV) than the value obtained in Pt/Fe_2O_3. In Pd/FeO_x and Pd/Al_2O_3, peaks centering at 335.7 and 335.1 eV are assigned to Pd^0, while 337.5 or 335.6 eV are typical values for Pd^{2+}. The shift of the binding energy of the Pd4$d_{5/2}$ peak to a lower value in FeO_x-supported Pd catalyst is also observed. These results demonstrate that the electronic environment of Pt and Pd over an FeO_x support is different from that of Al_2O_3 or Fe_2O_3-supported catalysts treated at higher temperatures, which is speculated to be caused by a strong metal–support interaction (SMSI) effect. As for the XP spectra of Fe2$p_{3/2}$ in FeO_x and Fe_2O_3-supported Pt, Pd catalysts, the situation is more complicated. Both Fe^0 and Fe^{2+} typical peaks could not be discerned, while the

Table 2
Kinetic parameters for CO oxidation over various supported Pt, Au, and Pd catalysts.

Catalyst	Loadings (wt%)	Method[a]	P_{CO}, P_{O2} (kPa)	T (range)[b] (°C)	E_a (kJ/mol)	r_M[c] ($mmol_{CO}\ g_M^{-1}\ s^{-1}$)	Surface metal atoms × 10^5 (mol g_{cat}^{-1})[d]	TOF × 10^3 (s^{-1})	Ref.
Pt/FeO_x	0.23	CP	1.0, air	27 °C 20–105 °C	33	0.16	–	–	This study
Pt/FeO_x	1.5	CP	1.0, air	27 °C 5–85 °C	30.4	0.13	1.3	151	This study
Pt/Al_2O_3	1.5	IM	1.0, air	130 °C 130–215 °C	115.5	0.05	2.2	34.2	This study
Pt/Al_2O_3	1.0	IM	5, 2.5 (N_2 balanced)	— >220 °C	120	Not stated	2.6[e]	Not stated	[29]
Pt/TiO_2	1.0	DP	1.0, air	27 °C 10–60 °C	49	1.4×10^{-4}	4.3[f]	2.7	[30]
Pd/FeO_x	1.9	CP	1.0, air	27 °C 5–80 °C	34.3	0.15	7.9	36.8	This study
Pd/Al_2O_3	1.4	IM	1.0, air	135 °C 90–220 °C	71.2	0.03	1.8	23.5	This study
Au/FeO_x	2.0	CP	1.0, air	27 °C –	–	0.61	–	400[g]	This study
Au/Fe_2O_3	3.15	CP	1.0, 1.0 (N_2 balanced)	30 °C –	31	0.16	2.9[f]	130	[31]
Au/TiO_2	0.5	DP	1.0, air	27 °C −20 to 70 °C	27	3.8×10^{-4}	0.8[f]	37	[30]

[a] CP: co-precipitation, IM: incipient wetness impregnation, DP: deposition–precipitation.
[b] There are a specific temperature and temperature range for each catalyst. The specific datum is the temperature at which the reaction rate (r_M) is obtained, while the E_a is measured in the temperature range.
[c] M: Pt, Pd, or Au.
[d] Obtained from CO chemisorption.
[e] Calculated from the given dispersion.
[f] Calculated from average particle size, assuming spherical particles.
[g] TOF normalized by the number of the surface noble metal atoms by an estimate of 30% Au dispersion.

oxidation state Fe^{3+} is dominated. Nevertheless, as XPS is a surface analysis technique and characterizations are performed under ex situ conditions, magnetite (Fe_3O_4), which is confirmed in XRD (see the next section), could not be distinguished in surface compositions is acceptable.

The surface atom ratios of Pt/Fe and Pd/Fe are also presented in Table 1. The surface atom ratio of Pt/Fe over Pt/FeO_x was 0.01, which was 0.6 times larger than the Pd/Fe ratio from loadings (assuming $x = 1.5$). This may be caused by a large amount of Fe^{3+} reduction simultaneous with the reduction of PtO_2 over Pt/FeO_x (see next section). Subsequently, more Pt species were possibly encapsulated with FeO_x and SMSI occurred. Moreover, this possible

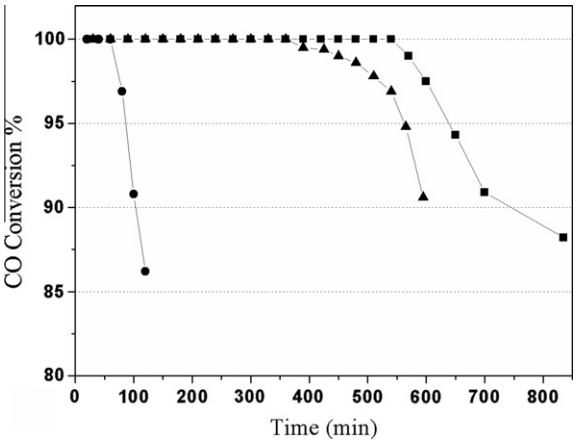

Fig. 2. Conversion of CO as a function of time over 1.5% Pt/FeO_x at 25 °C. Reaction conditions: 1% CO in air, SV = 15,000 ml h^{-1} g^{-1} (●); 1% CO in air, SV = 7500 ml h^{-1} g^{-1} (▲); 1% CO, 10% O_2, argon balance, SV = 7500 ml h^{-1} g^{-1} (■).

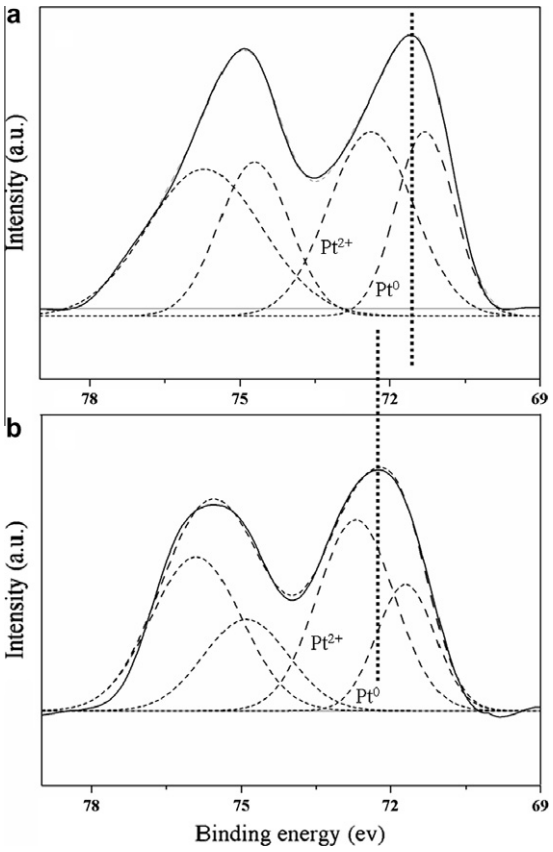

Fig. 3. XPS spectra (Pt4*f*) of supported Pt catalysts: (a) 1.5% Pt/FeO_x; (b) 1.6% Pt/Fe_2O_3.

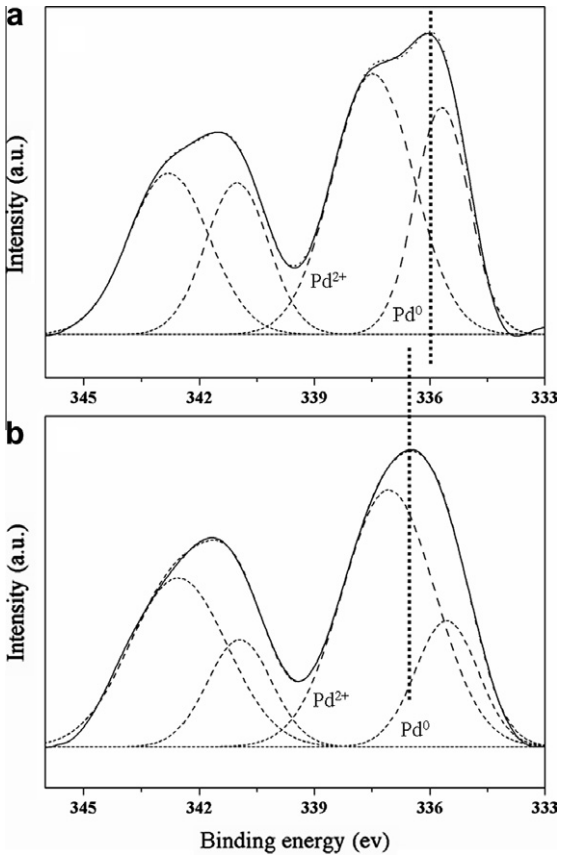

Fig. 4. XPS spectra (Pd3*d*) of supported Pd catalysts: (a) 1.9% Pd/FeO_x; (b) 1.4% Pd/Al_2O_3.

encapsulation effect of FeO_x may be a promotional effect on CO oxidation, as reported by Sun et al. [36]. A similar phenomenon was also observed in Pd/FeO_x. It has been reported that Fe oxide could interact strongly with Pt by modifying its electronic surface states [37]. The XPS results of Figs. 3 and 4, in which binding energy shifted to lower values support that Fe has a similar influence on Pt and Pd in FeO_x-supported catalysts. This electron transformation from Fe to Pt results in electron-rich Pt atoms and the shift of the Fermi level to a higher energy, which weakens the adsorption of CO [18]. A previous study demonstrated that the water–gas shift (WGS) reaction rate could be significantly enhanced by adding a monolayer of Fe_2O_3 (2%) in Pd/CeO_2 [38]. It was proposed that Fe could transfer oxygen from the iron oxide to the precious metal (Pd) and lower the barrier for oxygen transfer between CeO_2 and Pd, thereby enhancing the WGS reaction rate. The main requirement for this mechanism is that Fe_2O_3 must be in close contact with Pd on the surface. It is similar to the observations in this study. These observations might also be helpful in explaining the high activity of FeO_x-supported Pt and Pd catalysts in low-temperature CO oxidation.

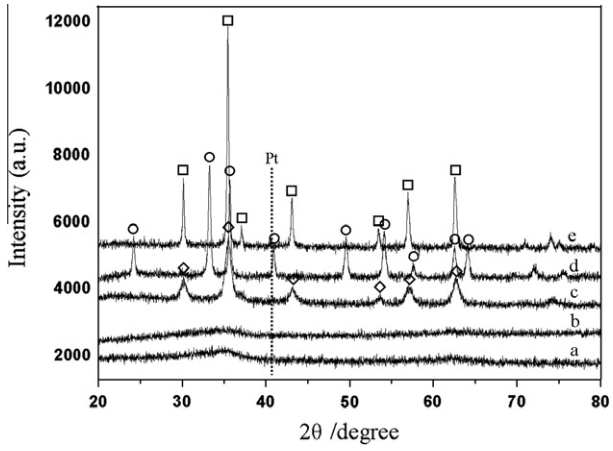

Fig. 5. X-ray diffraction patterns for supported Pt catalysts: (a) Fe(OH)$_x$, (b) Pt/Fe(OH)$_x$, (c) Pt/FeO_x, (d) Pt/Fe_2O_3-NR, (e) Pt/Fe_2O_3; hematite (○); magnetite (□, ◇).

XRD results (Fig. 5b) for Pt/Fe(OH)$_x$, just as for Fe(OH)$_x$ (Fig. 5a), show only two broad peaks at 35° and 62.5° (2θ), which are typical two-line ferrihydrite patterns, as can be expected from the conditions of the synthesis procedure [39]. This support, depending on drying temperature, is a mixture of amorphous FeO(OH,H_2O) and Fe_2O_3, as observed by Hermanek et al. [40]. However, crystalline magnetite (Fe_3O_4) was observed after the catalyst was reduced at 200 °C (Fig. 5c), indicating that the Pt species might be so active that Fe(OH)$_x$ could be partly reduced. It is worth pointing out that the characteristic peaks of ferrihydrite became faint after reduction, indicating that hydroxyl loss proceeded simultaneously with reduction of Fe_2O_3 to Fe_3O_4. Therefore, a large number of vacancies must be created, accompanied by hydroxyl removal to maintain the charge balance, and this would be helpful for the catalytic activity for CO oxidations over FeO_x-supported Pt, Pd. Meanwhile, the residual hydroxyls on the support were proposed to facilitate adsorption and activation of O_2 molecules in nearby oxygen vacancies by lowering the adsorption energy [41]. Additionally, Fig. 5c shows no evident characteristic diffraction peaks of Pt, indicating that Pt species in Pt/FeO_x are also highly dispersed even after reduction. α-Fe_2O_3 crystallite other than ferrihydrite was evident in Pt/Fe_2O_3-NR, indicating that hydroxyl in this catalyst has been removed in the calcination procedure. Typical magnetite (Fe_3O_4) diffraction peaks were also observed in Pt/Fe_2O_3, but the Fe modifying effect over Pt electronic state was different, as suggested by XPS characterization. Similar results were observed in FeO_x- and Fe_2O_3-supported Pd (not shown here).

To get explicit details of Pt particle size, two typical catalysts (1.5 wt% Pt/FeO_x and 1.5 wt% Pt/Al_2O_3) were examined with HRTEM, Fig. 6. No obvious Pt particles were observed over 1.5 wt% Pt/FeO_x, suggesting that Pt species were highly dispersed into or on the support, or more precisely, Pt species were in subnanometer cluster states. Meanwhile, the image showed that the support of 1.5 wt% Pt/FeO_x consisted of amorphous Fe(OH)$_x$ and Fe_3O_4, and the Fe_3O_4 crystal surface of (2 2 0) and (4 0 0) could be easily discerned. This is in good agreement with the XRD results. It is worth pointing out that an overlap of Fe_3O_4 (1 2 2) (*d*-spacing = 0.218) and Pt (2 0 0) (*d*-spacing = 0.196) crystal surfaces with weak contrast (enlarged region at the top right corner of Fig. 6a) could barely be recognized. It can be speculated that a partially crystalline structure of Pt began to form in a certain region, though the catalyst was not treated at high temperatures [42]. Moreover, those Pt species in subnanometer states probably also play an important role in catalytic performance, as suggested in early reports [43]. As for 1.5 wt% Pt/Al_2O_3, obvious Pt particles with size 1.7–2.7 nm and Al_2O_3 crystal surface of (0 1 2) were observed. Taking account of those results, particle size effects on catalytic performance cannot be ruled out at this stage.

3.3. TPR studies of supported Pt and Pd catalysts

H_2-TPR traces obtained over Fe(OH)$_x$- and Al_2O_3-supported Pt, Pd catalysts are shown in Fig. 7. Catalyst samples were first exposed to air (50 ml/min) for 1 h at selected temperatures for different catalysts before TPR. As can be seen from Fig. 7b, oxidic platinum in Pt/Fe(OH)$_x$ catalyst shows a characteristic TPR curve with a maximum reduction at 195 °C and a reduction tail up to

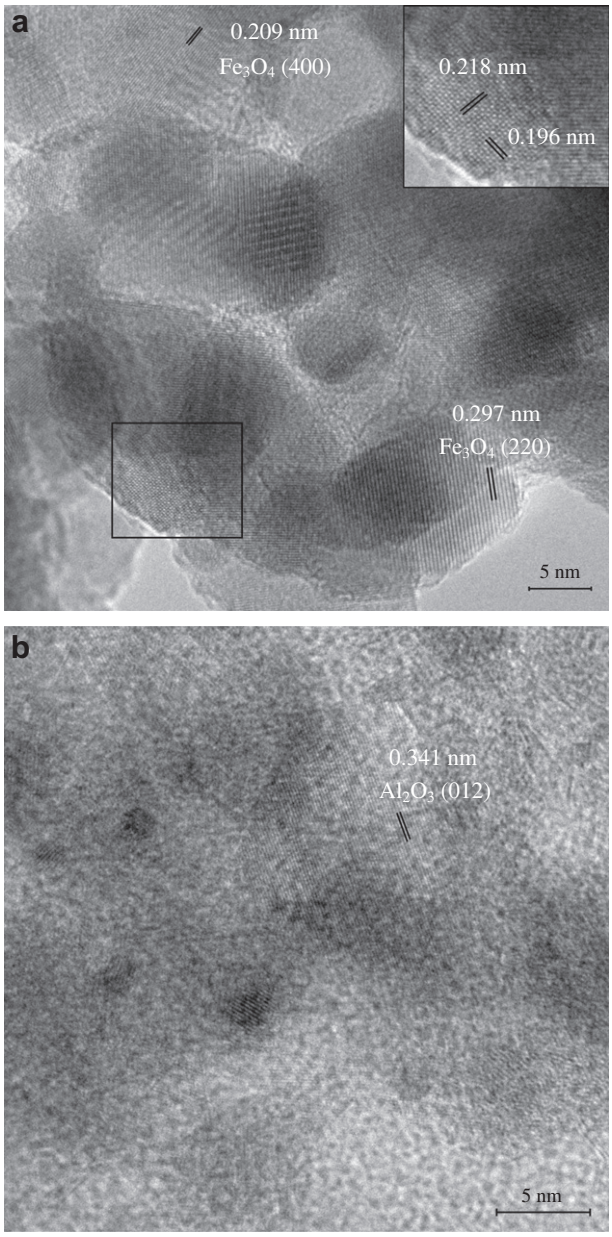

Fig. 6. Representative HRTEM images of (a) 1.5% Pt/FeO_x (inset: enlargement of the selected region) and (b) 1.5% Pt/Al_2O_3 catalysts.

about 500 °C. According to earlier report [44], the first peak was attributed to reduction of PtO_2 (Pt^{4+} was identified with XPS, 75.4 eV) and the broad peak located at high temperature to continuous reduction of Fe^{3+}. However, the total hydrogen consumed at the first peak (2.1 mmol g^{-1}) was 13 times larger than the corresponding consumption of Pt^{4+} to Pt^0 (0.15 mmol g^{-1}) in this catalyst, indicating that $Fe(OH)_x$ was reduced simultaneously. In addition, the residual amount of H_2 corresponds to 39% conversion of Fe^{3+} into Fe^{2+} in this catalyst. As for Pt/Al_2O_3-NR, only a small reduction peak with a maximum reduction at 230 °C was observed, which was different from the $Pt/Fe(OH)_x$ catalyst, and the H_2 consumption (0.14 mmol g^{-1}) corresponded fairly well to the total content of Pt. Similar results were also obtained over $Pd/Fe(OH)_x$ and Pd/Al_2O_3-NR catalysts. PdO reduction only accounted for 31% H_2 consumption in the first combined reduction peak over $Pd/Fe(OH)_x$, while excess H_2 equated to a reduction of 7.5% Fe^{3+} into Fe^{2+}. As for Pd/Al_2O_3-NR, a characteristic PdO reduction peak at 77 °C was observed, which was in agreement with early reports

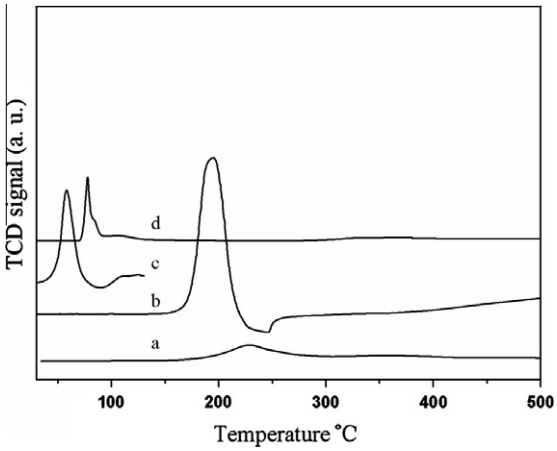

Fig. 7. H_2-TPR profiles of (a) Pt/Al_2O_3-NR, (b) $Pt/Fe(OH)_x$, (c) $Pd/Fe(OH)_x$, and (d) Pd/Al_2O_3-NR. Reduction conditions: 0.080 g sample, heated at a ramp of 10 °C/min from 25 °C to selected temperatures, 50 ml/min 5% H_2 in N_2.

[45]. Unlike $Fe(OH)_x$-supported Pt, Pd, no hydrogen spillover phenomena were observed over TPR traces of Pt/Al_2O_3-NR and Pd/Al_2O_3-NR, which might be caused by the inhabitation of chlorine from a chlorinated precursor [46]. No particles were detected in $Pt/Fe(OH)_x$ catalyst by HRTEM either before or after reduction in this manner. This puts at least a certain amount of particle size at ca. 1 nm or in the subnanometer range. It seems that those highly dispersed Pt and Pd clusters strongly facilitated the reduction of $Fe(OH)_x$ support, as Fe_2O_3 or $Fe(OH)_x$ without noble metals could not be reduced below 500 °C [47]. Meanwhile, a large number of Fe^{3+} can be reduced simultaneous with Pt and Pd in $Fe(OH)_x$-supported catalysts, particularly in Pt/FeO_x, indicating that there is strong interaction between Fe and Pt, Pd, which is in accordance with XPS results. Apart from amounts of vacancies created by hydroxyl loss in hydrogenation, the reduction readiness of $Fe(OH)_x$ would also facilitate the production of oxygen vacancies that are formed accompanied by induced support reduction from CO spillover as proposed by Bond et al. [48]. In the CO oxidation model involving support, it is believed that O_2 adsorption occurs on the support (or at the metal–support interface), possibly on oxygen vacancies. Furthermore, it should be present on semiconductor materials such as Fe_3O_4 and TiO_2, especially in the proximity of particles as a consequence of the Schottky junction at the metal–semiconductor interface [49]. It can be speculated that easily formed oxygen vacancies over Pt/FeO_x and Pd/FeO_x serve as the primary active site for O_2 activation, which leads to the availability of active oxygen for low-temperature CO oxidation over those catalysts.

Simultaneous reduction of 39% Fe^{3+} to Fe^{2+} would cause the increase in intensity of encapsulation, after which formation of Pt–Fe bimetal and corresponding SMSI might occur, as suggested by XPS. Those effects would cause the decrease in dispersion [28], which is in accordance with CO chemisorption results. So a relatively low dispersion of Pt over Pt/FeO_x obtained from CO chemisorption does not mean that Pt particles over this catalyst are large. Furthermore, Pt species are more likely highly dispersed in or over Pt/FeO_x, which is evidenced by XRD and HRTEM.

3.4. Investigation with chemisorptions

3.4.1. H_2–O_2 titration

Titration of chemisorbed O_2 by H_2 was used to further illustrate the active oxygen species as well as dispersion of Al_2O_3-, FeO_x-, and Fe_2O_3-supported Pt, Pd catalysts. Samples (80 mg) were first

Table 3
H_2–O_2 titration results over supported Pt, Pd catalysts.

Catalyst	H_2–O_2 titration (HOT-H_T)			H_2–O_2 titration (HOT-O_T)		
	Theoretic H_2 uptake (mmol g^{-1})	Actual H_2 uptake (mmol g^{-1})	Dispersion, *D*	Theoretic O_2 uptake (mmol g^{-1})	Actual O_2 uptake (mmol g^{-1})	Dispersion, *D*
1.5% Pt/FeO_x	0.12	0[a]	–	0.06	–	–
1.5% Pt/Al_2O_3	0.12	0.04	0.33	0.06	0.04	0.66
1.4% Pd/Al_2O_3	0.20	0.05	0.25	0.1	0.04	0.40
1.5% Pt/FeO_x	0.12	0.6	–	0.06	0.06	1.0
1.9% Pd/FeO_x	0.27	1.0	–	0.13	0.11	0.85
1.6% Pt/Fe_2O_3	0.12	0.05	0.42	0.06	0.05	0.83
2.1% Pd/Fe_2O_3	0.30	0.03	0.10	0.15	0.04	0.27

[a] Blank test, no prechemisorption step before titration.

reduced with H_2 and purged with highly pure N_2 for 1 h, and then cooled down to selected temperatures. Subsequently, samples were saturated with O_2 by titration and the saturated adsorption states were evidenced by MS signals as well as variation of catalyst bed temperatures. After being purged with N_2 for 0.5 h, the samples were titrated with H_2 to give HOT-H_T. Theoretic and actual H_2 uptakes as well as dispersion are compiled in Table 3. $Fe(OH)_x$ without Pt or Pd was first subjected to the HOT test. As expected, pure support had hardly any H_2 or O_2 uptake. A blank test without preadsorption of O_2 (blank HOT-H_T) over 1.5% Pt/FeO_x was also carried out, and hardly any H_2 consumption was observed. Those results indicate that H_2 and O_2 chemisorption could not occur over pure $Fe(OH)_x$, and physisorption can be neglected over this catalyst. Al_2O_3-supported Pt and Pd catalysts were subsequently subjected to HOT-H_T. H_2 uptake over 1.5% Pt/Al_2O_3 was 0.04 mmol g^{-1} and a dispersion of 0.33 with a mean particle size of about 3.4 nm was obtained. As for 1.4% Pd/Al_2O_3, the actual H_2 uptake was 0.05 mmol g^{-1} and a dispersion of 0.25 was obtained. Those results were in agreement with HRTEM characterization and early reports [50], indicating that the HOT characterization system we used was reliable. Interestingly, after incorporation of Pt and Pd over FeO_x, the actual H_2 uptake increased dramatically. H_2 uptake over 1.5% Pt/FeO_x was 0.6 mmol g^{-1}, four times more than in the theoretic account (0.12 mmol g^{-1}). A similar result was also observed over Pd/FeO_x. The actual H_2 uptake was 1.0 mmol g^{-1}, 3.7 times the theoretic amount (0.27 mmol g^{-1}). Both the O_2-saturated adsorption state and the H_2 titration terminal were confirmed by analyzing exhaust gas with MS. Also, HOTs over FeO_x-supported Pt and Pd catalysts were repeated three times to affirm those results, and the analytical data were reproducible within a 3% standard deviation. Due to its large amount, O_2 was not, at least not solely, adsorbed and activated on Pt or Pd. Instead, a large proportion of O_2 must have been located on the support. A similar phenomenon was also found over Au/$FeO_{1.5-x}$ catalyst after treatment at 400 °C in oxidative atmosphere and Au/CeO_2 [51,52]. Other than Au catalysts, Pt and Pd have stronger interaction with CO, which seriously restrains O_2 adsorption and activation over those active sites, resulting in low activity for CO oxidation at low temperatures. So offering active oxygen is more important for supported Pt and Pd catalysts. However, the abnormally high H_2 uptake disappeared after the $Fe(OH)_x$-supported Pt and Pd catalysts were calcined at elevated temperatures (500 °C). H_2 uptake was 0.05 mmol g^{-1} over 1.6% Pt/Fe_2O_3 (theoretic account: 0.12 mmol g^{-1}) with a dispersion of 0.42, which was similar to the results for Al_2O_3-supported Pt, Pd catalysts. Also, actual H_2 uptake over 2.1% Pd/Fe_2O_3 was only 0.03 mmol g^{-1}. In other words, O_2 could not be adsorbed and activated on those Al_2O_3 and high-temperature-treated Fe_2O_3 supports. The only active sites over those catalysts (Al_2O_3- and Fe_2O_3-supported Pt, Pd) for O_2 activation are Pt or Pd. So exclusive adsorption of CO over Pt, Pd at low temperatures and the incapability of Al_2O_3 and Fe_2O_3 to adsorb active O_2 make active oxygen unavailable for CO oxidation. Contrarily, partly reduced FeO_x support can offer active oxygen in the presence of Pt, Pd, making CO oxidation over Pt/FeO_x, Pd/FeO_x proceed over two adjacent but different active sites (Pt, Pd for CO and FeO_x for oxygen). Those results are in good agreement with the dramatic activity differences between Al_2O_3- (or Fe_2O_3-) and FeO_x-supported Pt, Pd in low-temperature CO oxidation. Also, the different reaction pathways between FeO_x- and Fe_2O_3-supported Pt, Pd at least partly explain why those two kinds of catalysts with similar E_a in quantity have dramatic differences in CO catalytic activities.

Since O_2 can be activated over FeO_x in the presence of Pt and Pd, O_2 titrations (HOT-O_T) of the chemisorbed H_2 over those catalysts were also tested (Table 3). As can be seen, neither FeO_x nor Fe_2O_3 and Al_2O_3 in the presence of Pt, Pd were able to activate H_2; that is, the amounts of chemisorbed H_2 calculated from HOT-O_T were

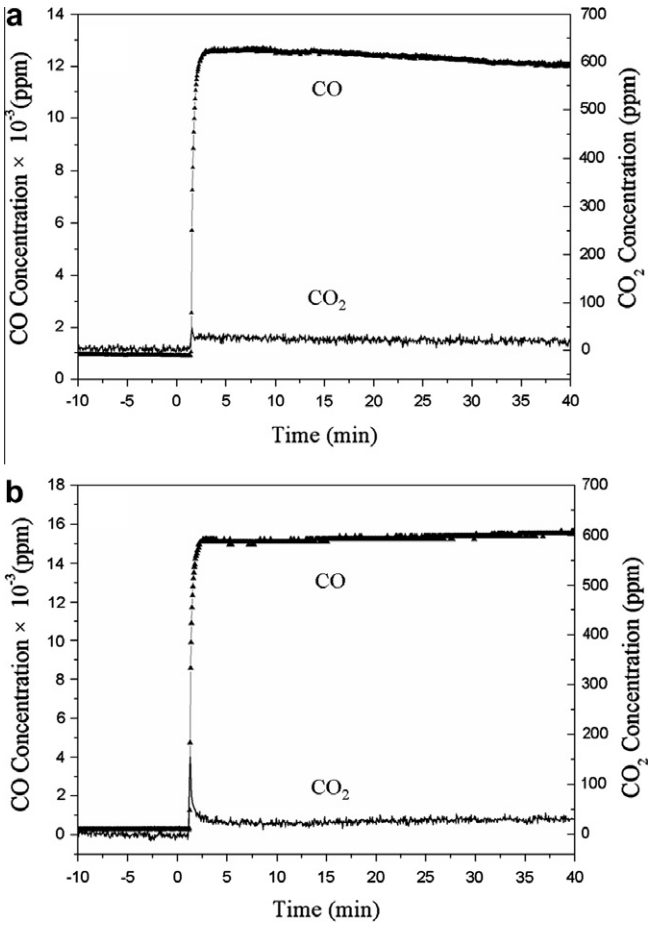

Fig. 8. CO_2 response for the reaction of (a) freshly reduced 1.5% Pt/Al_2O_3 with CO; (b) preadsorbed O_2 over 1.5% Pt/Al_2O_3 with CO.

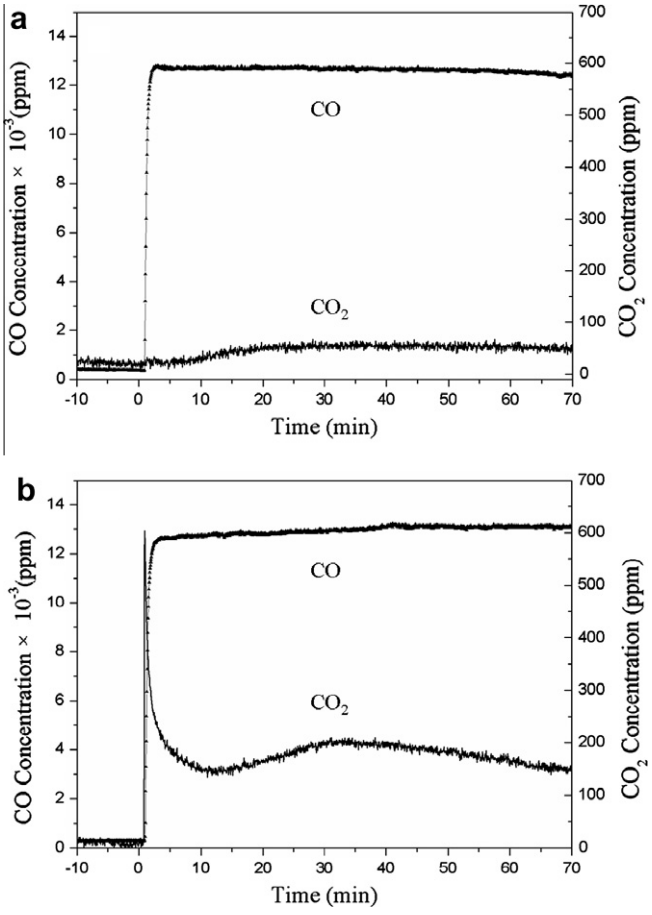

Fig. 9. CO_2 response for the reaction of (a) freshly reduced 1.5% Pt/FeO_x with CO; (b) preadsorbed O_2 over 1.5% Pt/FeO_x with CO.

normal. The actual O_2 uptake over 1.5% Pt/FeO_x was 0.06 mmol g^{-1} and the corresponding dispersion is 1.0. According to Scholten [53], even if dispersion is nearly one, the metal is not dispersed atomically. For instance, Pd crystallites with a diameter of 1 nm and containing about 63 Pd atoms have nearly 90% of their atoms at the surface. Considering the context of the present work, the values of dispersion =1 should imply that the Pt species over FeO_x is highly dispersed. The dispersions achieved in HOT-O_T were higher than the values obtained from HOT-H_T, and this may come from the readsorption of O_2 over FeO_x, as suggested by HOT-H_T and hydrogen spillover over Pt, Pd in the H_2 chemisorption step.

3.4.2. Time-resolved CO titration

In order to get a more explicit detail of oxygen active species and further evidence O_2 activation over specific FeO_x support, time-resolved CO titrations were carried out over Pt/Al_2O_3 and Pt/FeO_x catalysts. In this test, we concentrated on the amount of reactant species that can be adsorbed onto the catalyst and on possible differences in the timescale for CO_2 evolution. CO_2 evolution upon exposure to CO was followed by MS on-line analysis both for freshly reduced catalyst and for catalyst preexposed to oxygen. First, the measurement on 1.5% Pt/Al_2O_3 was carried out: an 80-mg sample was reduced in situ with 5% H_2/Ar and purged with deoxidized Ar at 300 °C for 1 h; 1% CO in Ar was introduced after the sample was cooled down to 150 °C without predosing oxygen. Meanwhile, CO and CO_2 responses were recorded, Fig. 8a. As can be seen, the very small CO_2 peak starts at 81 s, which would be considered a fast reaction. It has been suggested that lattice oxygen (O^{2-}) would cause a slow and broad CO_2 response [51]. So this narrow peak probably involves active oxygen species directly adsorbed onto Pt, while a trace of oxygen might come from the impurity of gas. For titration of the catalyst with oxygen preadsorption, 80 mg of Pt/Al_2O_3 was reduced and purged at 300 °C. After being cooled down to 150 °C, the sample was saturated with 1% O_2/Ar for 20 min and purged with Ar for 30 min in order to remove the residual gas-phase O_2. Subsequently, a stream of 1% CO/Ar was admitted to the system. As can be seen in Fig. 8b, the CO_2 peak started at 76 s, which probably resulted from a fast reaction of CO and preadsorbed oxygen on Pt particles. The calculated amount of adsorbed oxygen is about 1.2 μmol, which is slightly lower than the number of surface metal atoms (1.6 μmol, from CO chemisorption).

Titration of the 1.5% Pt/FeO_x sample without oxygen preadsorption was performed in a similar way, as mentioned earlier, except for the temperatures of reduction (200 °C for Pt/FeO_x) and titration (25 °C for Pt/FeO_x), Fig. 9a. As for the situation without preadsorption of oxygen, a small fraction of CO_2 response was not observed until 9.75 min after the introduction of 1% CO/Ar, which might be caused by the participation of lattice oxygen (O^{2-}) liberated during the partial reduction of Fe^{3+} to Fe^{2+}. In the comparative test (Fig. 9b), we preadsorbed oxygen (at 25 °C; 1% O_2/Ar for 20 min) on the reduced catalyst; after purging with Ar, 1% CO/Ar was introduced into the system. As can be seen, a fast (after 39 s) and sharp CO_2 response was observed in the first 15 min, which is dramatically different from the slow and broad response over the catalyst without oxygen preadsorption. More importantly, the calculated amount of adsorbed oxygen is ca. 3.5 times more than the total amount of Pt atoms (0.93 μmol, from CO chemisorption), indicating that a large proportion of oxygen adsorbs onto the support. It can be inferred from the relative high reaction rate that this active oxygen is not lattice oxygen (O^{2-}) but rather is in the form of superoxides (O_2^-). So O_2 might first combine with oxygen vacancies, which were produced together with hydroxyl loss and Fe^{3+} reduction as suggested by XRD and TPR, giving out active O_2^-. As was observed in electron spin resonance (ESR) measurements on supported Au catalyst [51,54,55]. The broad CO_2 peak with a maximum at 33 min might also come from the lattice oxygen from the support. Those results show clear evidence that a large amount of oxygen can adsorb and be activated on partly reduced FeO_x support in the presence of Pt, Pd, which is in accordance with the HOT characterization.

TPR profiles indicate that highly dispersed Pt, Pd facilitate $Fe(OH)_x$ reduction at relatively low temperatures, and a large number of vacancies are created, accompanied by hydroxyl removal to maintain the charge balance. The SMSI effect also becomes evident in the reduction procedure, as suggested by XPS and HRTEM. This leads to electron transfer from Fe to Pt and the shift of the Fermi level to higher energy, which weaken the adsorption of CO. Highly dispersed Pt, Pd species, probably in cluster states with the availability of many low-coordination Pt, Pd atoms, may also be helpful in CO oxidation. Nevertheless, most importantly, the H_2–O_2 titration and CO titration experiments presented here provide clear evidence that FeO_x support is involved in the CO oxidation, acting as an oxygen supply. Molecular oxygen adsorption on the support, probably on oxygen vacancies, explains both the fast CO_2 response and the large amount of active oxygen available for the reaction. This makes CO oxidation over Pt/FeO_x, Pd/FeO_x proceed over two adjacent but different active sites (Pt, Pd for CO and FeO_x for oxygen) with low activation energy. Hence, those catalysts have activities comparable to those of supported Au catalysts in low-temperature CO oxidation.

4. Conclusions

A FeO_x-supported Pt catalyst possessing activity (TOF of 151×10^{-3} s^{-1}, 1% CO balanced with air, atmospheric pressure, 27 °C) comparable to that of Au/FeO_x (400×10^{-3} s^{-1}, under the

same reaction conditions) in low-temperature CO oxidation was prepared. TPR, XRD, and HRTEM results show that Pt, Pd over $Fe(OH)_x$ can facilitate Fe^{3+} reduction and hydroxyl loss at relatively low temperatures, which leads to production of large numbers of oxygen vacancies. H_2—O_2 titration and time-resolved CO titration results show clear evidence that partly reduced FeO_x support is involved in the CO oxidation, acting as an oxygen supply. Thus, CO oxidation over Pt/FeO_x, Pd/FeO_x proceeds over two adjacent but different active sites (Pt, Pd for CO and FeO_x for oxygen) with low activation energies (30–34 kJ/mol), which accounts for the dramatic difference in activity from Al_2O_3- and Fe_2O_3-supported Pt, Pd. The contributions of SMSI and Pt, Pd particle size effect cannot be ruled out at this stage, but the existence of an oxygen reservoir on the FeO_x support probably reduces the dependence of catalytic activity on them. Those findings and the exploration of the mechanism may open up new routes in the search for high activity in low-temperature CO oxidation over supported noble metal catalysts, in particular for Pt and Pd.

Acknowledgment

This work was financially supported by the National Sciences Foundation of China (No. 20773146).

References

[1] X. Yu, S. Ye, J. Power Sour. 172 (2007) 145.
[2] M. Haruta, N. Yamada, T. Kobayashi, S. Iijima, J. Catal. 115 (1989) 301.
[3] A.A. Herzing, C.J. Kiely, A.F. Carley, P. Landon, G.J. Hutchings, Science 321 (2008) 1331.
[4] X. Xie, Y. Li, Z. Liu, M. Haruta, W. Shen, Nature 458 (2009) 746.
[5] M. Haruta, Gold Bull. 37 (2004) 27.
[6] A. Martínez-Arias, A.B. Hungría, M. Fernández-García, A. Iglesias-Juez, J.A. Anderson, J.C. Conesa, J. Catal. 221 (2004) 85.
[7] A. Bourane, D. Bianchi, J. Catal. 222 (2004) 499.
[8] E.Y. Ko, E.D. Park, H.C. Lee, D. Lee, S. Kim, Angew. Chem. Int. Ed. 46 (2007) 734.
[9] M. Kuriyama, H. Tanaka, S. Ito, T. Kubota, T. Miyao, S. Naito, K. Tomishige, K. Kunimori, J. Catal. 252 (2007) 39.
[10] P.S. Lambrou, P.G. Savva, J.L.G. Fierro, A.A. Efstathiou, Appl. Catal. B 76 (2007) 375.
[11] E.D. Park, D. Lee, H.C. Lee, Catal. Today 139 (2009) 280.
[12] Y. Ishida, T. Ebashi, S. Ito, T. Kubota, K. Kunimori, K. Tomishige, Chem. Commun. (2009) 5308.
[13] X. Mo, J. Gao, N. Umnajkaseam, J.G. Goodwin, J. Catal. 267 (2009) 167.
[14] A. Sirijaruphan, J.G. Goodwin, R.W. Rice, J. Catal. 224 (2004) 304.
[15] S.D. Ebbesen, B.L. Mojet, L. Lefferts, J. Catal. 246 (2007) 66.
[16] B. Kalita, R.C. Deka, J. Am. Chem. Soc. 131 (2009) 13252.
[17] A. Siani, O.S. Alexeev, B. Captain, G. Lafaye, P. Marecot, R.D. Adams, M.D. Amiridis, J. Catal. 255 (2008) 162.
[18] A. Siani, O.S. Alexeev, G. Lafaye, M.D. Amiridis, J. Catal. 266 (2009) 26.
[19] B. Qiao, L. Liu, J. Zhang, Y. Deng, J. Catal. 261 (2009) 241.
[20] S. Li, G. Liu, H. Lian, M. Jia, G. Zhao, D. Jiang, W. Zhang, Catal. Commun. 9 (2008) 1045.
[21] G.R. Heal, L.L. Mkayula, Carbon 26 (1988) 815.
[22] T.A. Dorling, R.L. Moss, J. Catal. 7 (1967) 378.
[23] K. Arnby, A. Törncrona, M. Skoglundh, Appl. Catal. B 49 (2004) 51.
[24] R.M. Finch, N.A. Hodge, G.J. Hutchings, A. Meagher, Q.A. Pankhurst, M.R.H. Siddiqui, F.E. Wagner, R. Whyman, Phys. Chem. Chem. Phys. 1 (1999) 485.
[25] L. Liu, B. Qiao, Z. Chen, J. Zhang, Y. Deng, Chem. Commun. (2009) 653.
[26] L. Liu, B. Qiao, Y. Ma, J. Zhang, Y. Deng, J. Chem. Soc. Dalton Trans. (2008) 2542.
[27] N.A. Hodge, C.J. Kiely, R. Whyman, M.R.H. Siddiqui, G.J. Hutchings, Q.A. Pankhurst, F.E. Wagner, R.R. Rajaram, S.E. Golunski, Catal. Today 72 (2002) 133.
[28] W. Rachmady, M.A. Vannice, J. Catal. 192 (2000) 322.
[29] U. Oran, D. Uner, Appl. Catal. B 54 (2004) 183.
[30] G.R. Bamwenda, S. Tsubota, T. Nakamura, M. Haruta, Catal. Lett. 44 (1997) 83.
[31] M.J. Kahlich, H.A. Gasteiger, R.J. Behm, J. Catal. 182 (1999) 430.
[32] V. Aguilar-Guerrero, B.C. Gates, Catal. Lett. 130 (2009) 108.
[33] L. Wang, X. Huang, Q. Liu, Y. Liu, Y. Cao, H. He, K. Fan, J. Zhuang, J. Catal. 259 (2008) 66.
[34] A. Sirijaruphan, J.G. Goodwin Jr., R.W. Rice, J. Catal. 227 (2004) 547.
[35] I. Meusel, J. Hoffmann, J. Hartmann, M. Heemeier, M. Bäumer, J. Libuda, H.J. Freund, Catal. Lett. 71 (2001) 5.
[36] Y. Sun, Z. Qin, M. Lewandowski, E. Carrasco, M. Sterrer, S. Shaikhutdinov, H.J. Freund, J. Catal. 266 (2009) 359.
[37] X. Liu, O. Korotkikh, R. Farrauto, Appl. Catal. A 226 (2002) 293.
[38] X. Wang, R.J. Gorte, Appl. Catal. A 247 (2003) 157.
[39] J.L. Jambor, J.E. Dutrizac, Chem. Rev. 98 (1998) 2549.
[40] M. Hermanek, R. Zboril, I. Medrik, J. Pechousek, C. Gregor, J. Am. Chem. Soc. 129 (2007) 10929.
[41] Z. Zheng, J. Teo, X. Chen, H. Liu, Y. Yuan, Eric, R. Waclawik, Z. Zhong, H. Zhu, Chem. Eur. J. 16 (2010) 1202.
[42] T. Akita, M. Okumura, K. Tanaka, M. Kohyama, M. Haruta, Catal. Today 117 (2006) 62.
[43] Y. Sun, L. Zhuang, J. Lu, X. Hong, P. Liu, J. Am. Chem. Soc. 129 (2007) 15465.
[44] E. Rogemond, R. Fréty, V. Perrichon, M. Primet, S. Salasc, M. Chevrier, C. Gauthier, F. Mathis, J. Catal. 169 (1997) 120.
[45] E.C. Hsiao, J.L. Falconer, J. Catal. 132 (1991) 145.
[46] S. Bernal, F.J. Botana, J.J. Calvino, M.A. Cauqui, G.A. Cifredo, A. Jobacho, J.M. Pintado, J.M. Rodriguezizquierdo, J. Phys. Chem. 97 (1993) 4118.
[47] P.S. Lambrou, A.M. Efstathiou, J. Catal. 240 (2006) 182.
[48] G.C. Bond, L.R. Molloy, M.J. Fuller, J. Chem. Soc. Chem. Comm. (1975) 796.
[49] J.C. Frost, Nature 334 (1988) 577.
[50] J. Freel, J. Catal. 25 (1972) 149.
[51] M.M. Schubert, S. Hackenberg, A.C. van Veen, M. Muhler, V. Plzak, R.J. Behm, J. Catal. 197 (2001) 113.
[52] D. Widmann, R. Leppelt, R.J. Behm, J. Catal. 251 (2007) 437.
[53] J.J.F. Scholten, Stud. Surf. Sci. Catal. 3 (1979) 685.
[54] H. Liu, A.I. Kozlov, A.P. Kozlova, T. Shido, K. Asakura, Y. Iwasawa, J. Catal. 185 (1999) 252.
[55] M. Okumura, J.M. Coronado, J. Soria, M. Haruta, J.C. Conesa, J. Catal. 203 (2001) 168.